Stress-Strain Behaviour and Model Prediction of Reinforced Residual Soil

S.A. Mofiz & M.M. Rhaman
Department of Civil Engineering, Rajshahi University of Engineering Technology, Rajshahi 6204, Bangladesh
samofiz@hotmail.com

M.A. Alim
Department of Civil & Environmental Engineering, Saitama University, 645 Shimo-okubo, Saitama-shi Saitama, 338 8571, Japan
s03kc026@post.saitama-u.ac.jp

Abstract: A study of the shear strength and deformation characteristics of unreinforced and geosynthetic reinforced residual soil is presented. Direct shear testing was conducted using a computerized shear box apparatus with stress levels ranging between 0.05 to 0.40 MPa. Effects of nonwoven geotextile reinforcement, orientation of reinforcements and volume changes on the shear strength of soil composites were analyzed. For reinforced soil composites, it was observed that the shear and volume change behaviour is related to the degree of reinforcement orientation. It was also showed that the contraction or dilation properties of the unreinforced and reinforced soil composites are highly dependent on the stress levels. An elasto-plastic model with plastic hardening (load transfer model) was extended to incorporate cohesive soils. The model parameters were then used to predict the stress strain behaviour of unreinforced and reinforced soil. The results presented satisfactory agreement with experimental observations at higher stress levels.

1 INTRODUCTION

In recent years, the practice of using plastic grids, geosynthetic fabrics and metal strips to increase shear resistance and stiffness of soils has become widespread (Mitchell 1981). Uses of geosynthetics to increases the bond in the soil system due to the interlocking of the soil particles with the reinforcement aperture as well as enhancing the bearing resistance of the transverse members of the reinforcement. Effectiveness of the reinforcements in contributing an increase in the shear resistance is highly dependent on the orientation of reinforcements with respect to the failure plane. Most studies and design methods and charts are well established on the use of granular soils. In tropical countries, the locally available residual soil is too plentiful to be ignored. Furthermore, in terms of cost and use of locally available materials will result in the reduction of the cost of construction. However, the interaction mechanism of the reinforced residual soil and the mobilization of the tensile strain in the reinforced composites are not yet well understood due to limited study. A limited amount of information is presently available on studies related to reinforced clay with plastic reinforcement under different drained conditions (Ingold, 1983; Ingold & Miller, 1983). Several successive geosynthetic applications have presented the potential of using c-ϕ type soils as backfill materials (Delmas *et al.*, 1992; Tatsuoka *et al.*, 1996). As a result of the growing interest in utilizing such soils in reinforced soil structures, research on the subject of the geosynthetic-cohesive soil interface behaviour has been intensified (Athanasopoulos, 1996). For the reasons mentioned above, a thorough investigation of the stress-deformation and soil reinforcement interaction on a residual soil was conducted. An elasto-plastic model (load transfer model) assuming strain hardening behaviour was used to characterize its stress-deformation and contraction-dilation of reinforced soil. The experimental test results were adopted to determine the model constants. The shear stress-displacement and volume change characteristics of the reinforced residual soil composites were analyzed. The experimental results were compared to that of the model predicted results.

2 SAMPLE PREPARATION AND TESTING PROGRAM

The residual soil used in this work is classified as CH in the Unified Soil Classification System (USCS) having specific gravity G_s = 2.63, liquid limit LL= 73% and plastic limit PL = 39%, γ_d = 14.42 kN/m^3 and w_{opt} = 24.6 %. In this study, a non-woven geotextile (Polyfelt TS 60) was used as the reinforcement material. The tensile strength properties of the reinforcement were determined following ASTM D4595- (ASTM 2000). The physical and mechanical stress-strain properties of the nonwoven geotextile are summarized in Table 1.

Table 1. Physical and mechanical properties of the nonwoven geotextile.

Material properties	Value
Thickness at 2 kPa	2.25 mm
Mass	245 g/m^2
Tensile strength (machine direction)	18.68 kN/m
Tensile strength (cross direction)	19.12 kN/m
Elongation (machine direction)	74 %
Elongation (cross direction)	51 %

The moist soil was compacted in a shear box mould by machine compaction to the desired height and unit weight at the optimum moisture content. In the case of reinforced soil, the reinforcement consisted of 100 mm x 60 mm size fabric that was cut from the sheet and placed inside the soil in different orientations. Four series of tests were carried out on both the unreinforced and

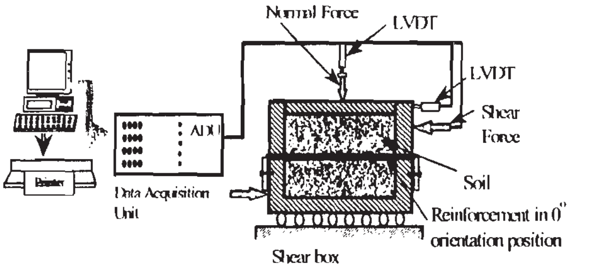

Fig. 1. Computer controlled experimental setup of the direct shear test (Mofiz, 2000).

reinforced residual soil at normal pressures varying between 0.05 - 0.40 MPa and the strain rate of 0.25 mm/min. The tests were conducted on ELE computer controlled shear box equipment using load-deformation transducers and data-logging system is shown in Fig. 1.

3 ELASTO-PLASTIC MODEL

Juran *et al.* (1988) proposed a soil-reinforcement load transfer model assuming an elasto-plastic strain hardening behaviour for sand and an elastic-perfectly plastic behaviour of the reinforcement. In this elasto-plastic model, the soil is considered homogeneous, isotropic, and strain hardening behaviour. In the analysis of direct shear test results, it is convenient to consider the shear strain as a strain hardening parameter $\gamma_{xy} = \gamma$. In this study the concept was extended to incorporate cohesive soil which can be readily applied to residual soils.

The yield function is defined by using the Mohr-Coulomb type yield function and can be expressed as

$$f\left(\sigma_{ij}, c, \gamma_{xy}\right) = \frac{\tau_{xy}}{\sigma_y} - \frac{c}{\sigma_y} - S(\gamma_{xy}) = 0 \qquad (1)$$

where τ_{xy} is the shear stress, σ_y is the applied normal stress, c is the cohesion intercept, and the $S(\gamma_{xy})$ function is the related to the $h(\gamma)$ function which is a hyperbolic function. The schematic diagrams of the strain hardening function and volumetric strain for both loose and dense soil as shown in Fig. 2.

The stress ratio-dilatancy rate for both contracting and dilating soils are also shown in the figure. The maximum plastic dilatancy rate, $\eta_{min} = min(d\varepsilon_v/d\gamma)$ is approximately equal to the slope of the volumetric strain-shear curve at the peak of the stress-strain curve, whereas the dilatancy rate at the residual (critical) state is equal to $\eta = 0$. This soil model needs five parameters i.e., G/σ_n which is the ratio of the initial shear modulus to the normal stress, ϕ is the friction angle, ϕ_c is the critical state friction angle of the soil, μ_1 and μ_2 are the contracting and dilating correction factors which is defined in Fig. 2. All these parameters may be determined from the analysis of either direct shear test or conventional triaxial test results. It should be noted that these soil properties are functions of the applied normal stress at the interface, soil density and moisture content. Therefore the average characteristics of the compacted residual soil to a given maximum standard Proctor density were used to represent its behaviour in each specified range of normal stresses.

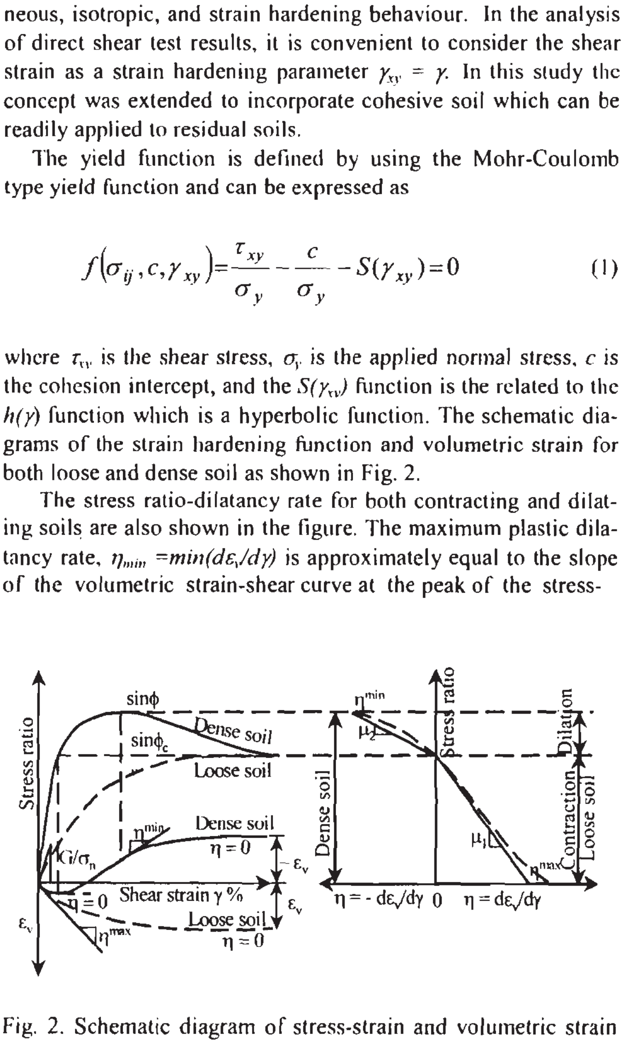

Fig. 2. Schematic diagram of stress-strain and volumetric strain characteristics of load transfer model.

For loose soil, the strain hardening or softening function $h(\gamma)$ is a hyperbolic function and can be expressed as:

$$h(\gamma) = \frac{\gamma}{(a + b\gamma)} \qquad (2)$$

The two constants a and b can be evaluated from the experimental data of the direct shear test in which $a = \sigma_n/G$, and $b = 1/tan\phi_{cv}$.

For the case of medium to high density soils, it is assumed that the hardening function $h(\gamma)$ is a parabolic function and can be written as:

$$h(\gamma) = \frac{F\gamma(\gamma - a)}{(\gamma + b)^2} \qquad (3)$$

where the constants F, a and b are determined from the following equations for the direct shear test: $F = tan\ \phi_{cv}$, $a = -4(\sigma_n/G)(tan^2\phi\ l^2)/tan\phi_{cv}$ and $b = 2(\sigma_n/G)(tan\ \phi\ l)$ with $l = 1 + [1 - \{tan\ \phi_{cv}/tan\phi\}]^{1/2}$.

4 RESULTS AND DISCUSSIONS

Test results of unreinforced and reinforced soil with different normal stresses are presented in Figs. 3 and 4. The shear stress- and shear displacement plot indicates that the relative shear displacement corresponding to maximum shear stress increases with interface normal stress. The shear stress and shear displacement of all unreinforced and reinforced samples at the initial shearing were similar since the effect of the reinforcement will only begin to function at some finite shear displacement. The result shows different strain pattern at higher displacement when the soil samples started to dilate.

The results of unreinforced and reinforced soil samples also show that dilatancy is dependent on the normal stress. The best fit straight line failure envelope in Fig. 5(a) indicates a cohesive-frictional behaviour with strength parameters in terms of total stresses for unreinforced soil in which $\phi = 29.03^{\circ}$, $c = 100.6$ kPa and for reinforced soil: $\phi_r = 32.95^{\circ}$, $c = 118.46$ kPa, respectively. A comparison between unreinforced and reinforced soil with respect to the peak shear stress versus normal interface stress with different reinforcement orientations can be deduced from Fig. 5(b). From this figure it is observed that the failure envelope of the unreinforced soil exhibit linear behaviour whereas a curvilinear or bilinear behaviour is illustrated for reinforced soil. This behavior is in agreement with the results published by other researchers (eg. Ranjan et al., 1996 and Athanasopoulos, 1996). The model constants obtained from plots of direct shear test results for unreinforced and reinforced soils are presented in Table 2.

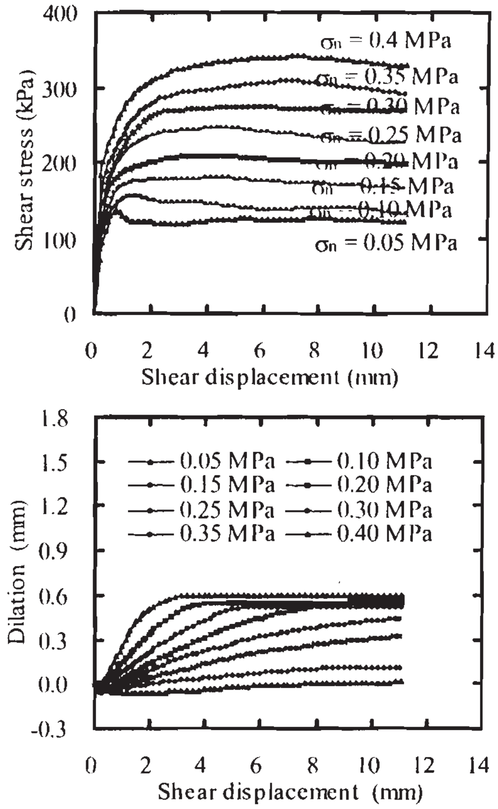

Fig. 3. Stress vs. shear deformation and dilation vs. shear deformation of unreinforced soil.

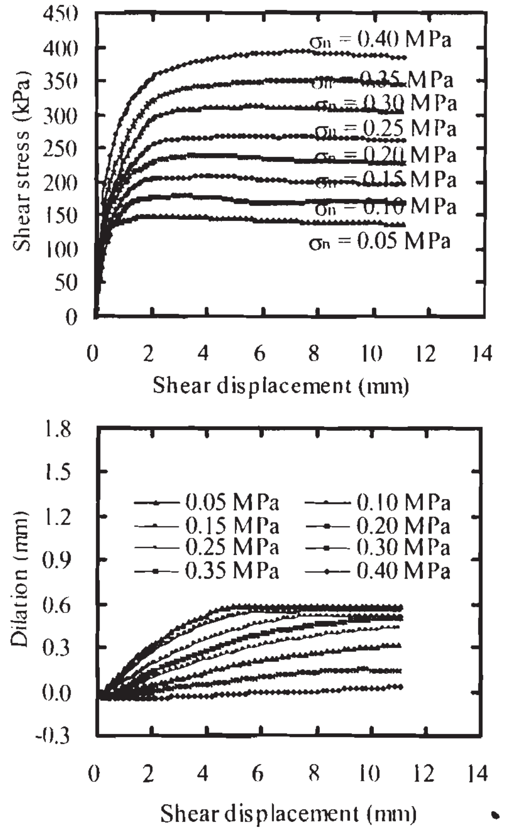

Fig. 4. Stress vs. shear deformation and dilation vs. shear deformation of reinforced soil.

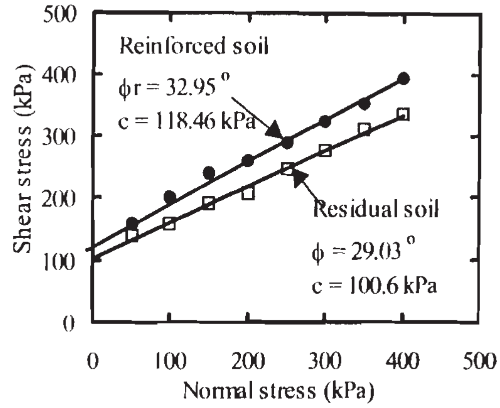

Fig. 5(a). Best fit failure envelope of unreinforced and reinforced soil.

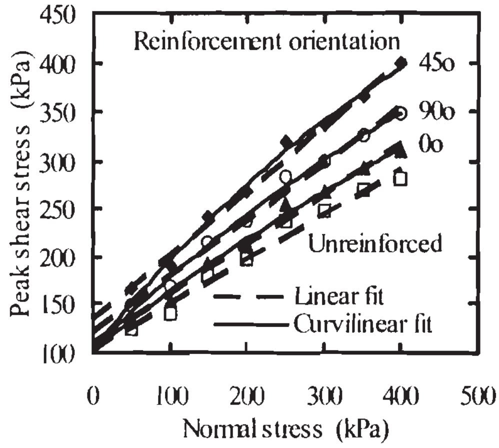

Fig. 5(b). Comparison of failure envelopes of the unreinforced and reinforced soil.

Table 2. Load transfer model parameters for unreinforced and reinforced soil.

Model parameters	Soil types	
	Unreinforced soil	Reinforced soil
G/σ_n	85.68	72.65
c	100.6 kPa	118.46 kPa
ϕ	29.03°	32.95°
ϕ_{cv}	28.18°	30.62°
μ_1	2.46	3.16
μ_2	3.48	4.10

The predicted responses of the load transfer model (elasto-plastic model) of shear displacement versus stress ratio and measured shear stress-displacement versus stress ratio for unreinforced and reinforced soils are presented in Figs. 6 (a) and (b). The stress-strain responses for reinforced soil are better than that of unreinforced soil especially for higher normal pressures. The trend of predicted curve for different interface normal stress values is in fare agreement with the test data at small displacements. The prediction is also good for higher normal stresses compared to cases at lower normal stresses since the unreinforced and reinforced soil shows a distinct strain softening behaviour.

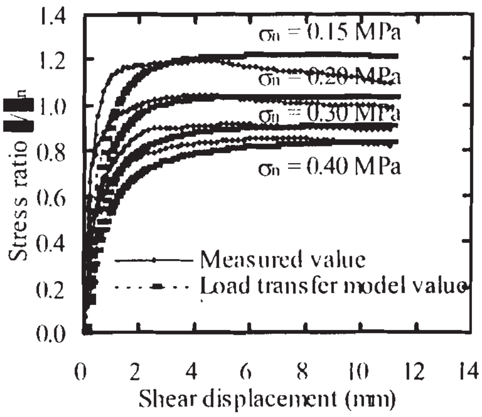

Fig. 6(a). Measured and predicted responses of shear displacement versus stress ratio of the unreinforced soil.

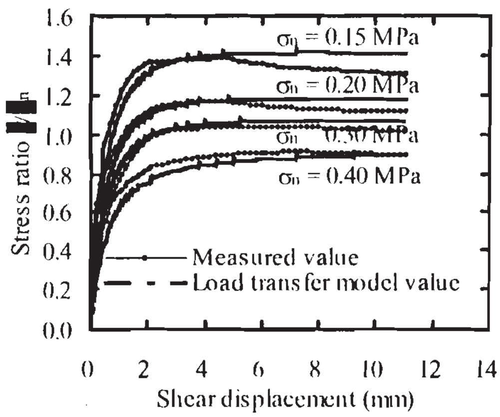

Fig. 6(b). Measured and predicted responses of shear displacement versus stress ratio of the reinforced soil.

5 CONCLUSIONS

The following observations and conclusions can be made on the basis of the work presented as follows:

1. To examine the stress-strain characteristics of unreinforced and reinforced granite residual soil a testing program was carried out in a modified direct shear apparatus.

2. Test results showed that the reinforcement inclusion significantly increases the ultimate shear strength. The composite soils system also fails at relatively larger shear displacement and in most of the cases the reinforced soil shows a strain hardening behaviour.

3. It was observed that the shear strength increases with the reinforcement orientation, and it was more effective when the orientation was 45° to the shear plane.

4. Failure of the composite soil system may be of two different patterns indicated by a linear or bilinear/curvilinear failure envelope.

5. The load transfer model of Juran *et al.* (1988) was extended for the case of cohesive soil and was tested for its validity for the residual soil.

6. Prediction using the model constants provides good agreement with the experimental results particularly for reinforced soil at high normal stresses.

REFERENCES

Athanasopoulos, G.A. 1996. Results of direct shear tests on geotextile reinforced cohesive soil. *Geotextiles and Geomembranes* 14: 619-644.

ASTM 2000. Testing of geotextiles related products. *Annual Book of ASTM Standards, Vol. 04.08, D4595*, American Society Testing & Materials.

Delmas, Ph., Gotteland, J.P., & Haidar, S. 1992. Two full size structures reinforced by geotextiles. *In Grouting, Soil Improvement and Geosynthetics, ASCE, Geotechnical Special Publication No.30*, Eds. 2: 1201-1212R.H. Borden, R.D. Holtz and I. Juran.

Ingold, T.S. 1983. Reinforced clay subject to undrained triaxial loading. *Journal of Geotechnical Engineering, ASCE* 109: 738-744.

Ingold, T.S., & Miller, K.S. 1983. Drained axisymmetric loading of reinforced clay. *Journal of Geotechnical Engineering, ASCE* 109: 838-898.

Juran, I., Guermazi, A., Chen, C.L. & Ider, M.H. 1988. Modelling and simulation of load transfer in reinforced soil: Part I. *International Journal of Numerical Analytical Methods in Geomechanics* 12: 141-155.

Mofiz, S.A. 2000. Behaviour of unreinforced and reinforced residual granite soil, Ph.D. Thesis, University Kebangsaan Malaysia: 315.

Mitchel, J.K. 1981. Soil improvement: state of the art, state of the art rep., session 12. *Proceedings 10th International Conference on Soil Mechanics and Foundation Engineering*, Stockholm, Sweden.

Tatsuoka, F., Uchimura, T., Tateyama, M. & Koseki, J. 1996. Geosynthetic-reinforced soil retaining walls as important permanent structures, Geosynthetic: Applications, Design and Construction. *Proceedings of the 1st European Geosynthetic Conference*: 3-24. Maastricht, The Netherlands.

Ranjan, G., Vasan, R.M., & Charan, H.D. 1996. Probabilistic analysis of randomly distributed fiber-reinforced soil. *Journal of Geotechnical Engineering, ASCE* 122(6): 419-426.